Comput. Math. Applic. Vol. 13, No. 1–3, pp. 111–121, 1987
Printed in Great Britain.

0097-4943/87 $3.00 + 0.00

AIRCRAFT PURSUIT–EVASION PROBLEMS WITH VARIABLE SPEEDS

U. R. PRASAD
School of Automation, Indian Institute of Science, Bangalore, India

N. RAJAN
Sterling Software, Palo Alto, CA 94043, U.S.A.

Abstract—Aircraft pursuit–evasion encounters in a plane with variable speeds are analysed as a differential game. An engagement-dependent coordinate system confers open-loop optimality on the game. Each aircraft's optimal motion can be represented by extremel trajectory maps which are independent of role, adversary and capture radius. These maps are used in two different ways to construct the feedback solution. Some examples are given to illustrate these features. The paper draws on earlier results and surveys several existing papers on the subject.

1. INTRODUCTION

The scope of air combat studies is wide-ranging—from the influence of initial conditions (role selection problem) aircraft performance and weapon system capability (including maneuverability/weapon radius tradeoffs) upon the combat outcome to the development of idealized tactics for onboard flight path management. Analyses of combat encounters between two aircraft are complex because of the high order and nonlinear nature of aircraft dynamics and variability in modeling the termination and criterion functions. A differential game model of the problem follows naturally from the total opposition of the adversaries and their capabilities not being widely different. A feedback saddle point solution is absolutely essential for each player in a game to take advantage of possible nonoptimal play by the opponent. Deterministic formulations with complete and perfect information to the participants have produced several useful results. Past analyses of aircraft pursuit–evasion have simplified the situation along different lines.

In the first approach [1–9], combat encounters between aircraft have been studied with the aircraft assumed to fly at constant speed with a variety of terminations to reflect weapon system characteristics and/or role selection aspects (variants of the Two Car Game of Isaacs). The main advantages are a reduced game dimension (three-dimensional) and analytical integration of the canonical (retrogressive path) equations. The optimal paths are composed of circular arcs and straight line segments. This class of problems exhibits a rich variety of singular surfaces. These are constructed without any need to iterate on the terminal parameters. Although several interesting and useful results have been obtained, the constant speed assumption is not realistic as modern aircraft exhibit large variations in speed and altitude during combat.

The second approach [10–14] relies on computational techniques to solve the two-point boundary value problem for determining the optimal controls at a given initial state. Difficulties associated with the construction of discontinuous and exceptional game surfaces have been obviated by resorting to a fixed "finite-horizon" miss distance formulation. The state space is discretized and the aircraft models simplified to keep the computational effort at a practical level in obtaining a "near-optimal" solution.

The third approach uses the energy state models or other forms of order reduction for the aircraft. In differential turning chases [15–18] each aircraft is described by its heading and specific energy. The relative positions of the aircraft are suppressed to keep the game dimension at three. Forced singular-perturbation techniques [19–22] use the time-scale separation inherent in some aircraft maneuvers to reduce the order of the problem. An approximate feedback guidance law suitable for onboard implementation can be obtained by this approach. These methods are limited by the assumptions made in separating the time scales. The domain of validity of the solution can be determined by comparison with exact solutions. Considerable scope for future work exists here.

Compared to the three-dimensional pursuit–evasion discussed above, variable speed pursuit–evasion in a plane [23–27] uses more exact point-mass models for the aircraft and exploits the features of the pursuit–evasion class of differential games to the fullest extent. The pursuit–evasion differential games studied here exhibit separate dynamics for the combatants with termination defined in terms of their relative position and orientation and with payoff involving capture time. This paper presents some of the highlights of this research as the planar analysis is a necessary step towards the ultimate solution of the three-dimensional problem.

The paper is organized as follows. Section 2 presents the solution in the small of the variable speed pursuit–evasion differential game in terms of the concept of maps of extremal trajectories. Section 3 discusses the construction of such maps for realistic aircraft. Section 4 is addressed mainly to the feedback solution of the game and the construction of the game surfaces. Section 5 gives some examples of Barrier and Dispersal points. The major results can be summed up as the applicability of the map of extremal trajectories to an aircraft generally regardless of its role, adversary or capture radius and the ability to obtain the feedback solution for different values of capture radius and interchange of roles with very little additional effort.

2. THE CONCEPT OF THE EXTREMAL TRAJECTORY MAP (ETM)

The motion of the pursuer (P or generally Aircraft 1) and evader (E or generally Aircraft 2) is governed for $i = \mathrm{p}, \mathrm{e}$ or $1, 2$ by the equations

$$\dot{x}_i = \mathrm{M}_i \cos \beta_i, \tag{1}$$

$$\dot{Y}_i = \mathrm{M}_i \sin \beta_i \tag{2}$$

$$\dot{\mathrm{M}}_i = A_i(\mathrm{M}_i)\,\Pi_i - B_i(\mathrm{M}_i) - C_i(\mathrm{M}_i)\omega_i^2, \tag{3}$$

$$\dot{\beta}_i = f_i(\mathrm{M}_i)\omega_i, \tag{4}$$

subject to the state-variable constraint on the Mach number M_i,

$$\mathrm{M}_i \epsilon [\underline{\mathrm{M}}_i, \bar{\mathrm{M}}_i] \tag{5}$$

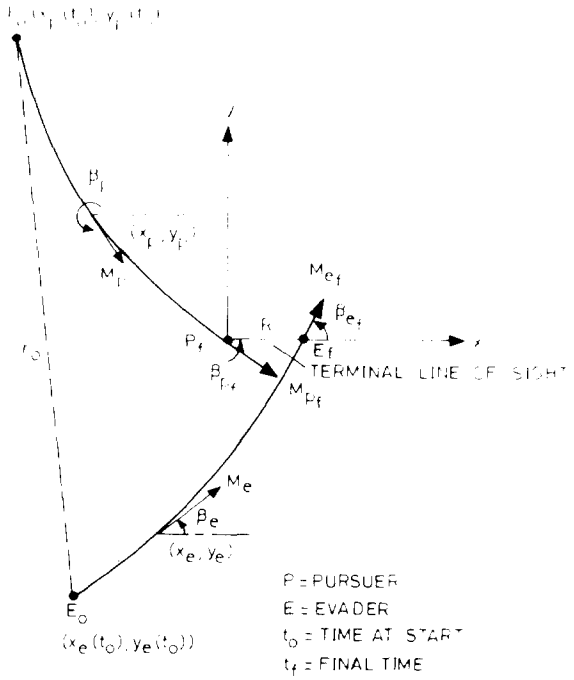

Fig. 1. The coordinate system.

with the throttle setting Π_i and the bank control ω_i satisfying

$$\Pi_i \epsilon [0, 1] \tag{6}$$

$$\omega_i \epsilon [-1, 1]. \tag{7}$$

The model is first given in [23]. The vector (x_i, y_i) represents the position of aircraft i in any convenient coordinate system in the plane. The heading β_i is measured relative to the x-axis. The functions f_i, A_i, B_i, and C_i represent the maximum instantaneous turn rate, the maximum thrust, the zero-bank drag and the lift-induced drag respectivley.

Capture is said to occur when the evader is brought within the circular capture set centred at the pursuer with radius R and the line of sight is shrinking. The payoff is the time to capture which is minimized (maximized) by the pursuer (evader).

The coordinate axes are selected to be engagement-dependent with the origin at the pursuer's (or evader's) position at capture and the x-axis in the direction of the terminal line of sight (Fig. 1). This leads to a decoupling of the canonical equations (which constitute the differential game solution in the small) into two disparate sets (one for each aircraft) confering an open loop optimality on both.

Each aircraft's extremal trajectory map (ETM) is obtained by retro integration of its canonical system comprising (1)–(4) and the equation for its speed adjoint p_{M_i}

$$\dot{p}_{M_i} = \cos \beta_i + y_i \mathrm{d}\dot{\beta}_i/\mathrm{dM}_i - p_{M_i} \mathrm{d}\dot{M}_i/\mathrm{dM}_i \tag{8}$$

for different values of the terminal velocity vector (M_f, β_f). The remaining terminal conditions are zero. The optimal controls Π_i and ω_i in (1)–(4), (8) are given by

$$\left.\begin{aligned} &\Pi_i = 1 \\ &\omega_i = \mathrm{sat}\{-f_i y_i/[2\, C_i\, (p_{M_i} + \bar{\mu}_i)]\} \end{aligned}\right\} \quad \text{for } p_{M_i} + \bar{\mu}_i < 0 \tag{9}$$

$$\left.\begin{aligned} &\Pi_i = 0 \\ &\omega_i = \mathrm{sgn}(y_i) \end{aligned}\right\} \quad \text{for } (p_{M_i} + \bar{\mu}) > 0 \tag{10}$$

here $\bar{\mu}_i$ is the Kuhn–Tucker multiplier accounting for (5).

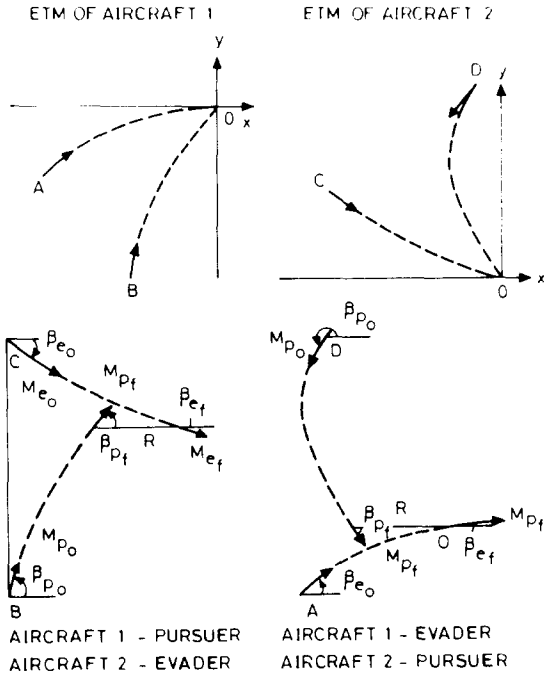

Fig. 2. Piecing encounters from ETMs.

The identical form of the canonical systems implies that the ETM is essentially independent of role, adversary and capture radius. That the same ETM applies for the aircraft in an interception role is explicitly shown in [26]. In this case, the evader's role is passive and uses an open loop strategy under no information about the pursuer's location. The pursuer uses a feedback strategy under advance knowledge of evader's actions. All extremal trajectories that the aircraft may use in any time optimal pursuit–evasion–interception encounters against any adversary are present in its ETM. The ETM thus offers a framework to represent the optimal performance of a combat aircraft.

Given the ETMs of two aircraft, a pair of extremals (one from each map) can be put together to yield a candidate pursuit–evasion encounter (Fig. 2). If the distance between the two aircraft at termination is R and is shrinking, i.e.

$$\mathrm{M}_{\mathrm{p}_f} \cos \beta_{\mathrm{p}_f} - \mathrm{M}_{\mathrm{e}_f} \cos \beta_{\mathrm{e}_f} < 0. \tag{11}$$

the pursuit–evasion encounter so generated retrogressively is optimal in feedback sense only until a singular surface such as the Barrier or a Dispersal surface is met with. The construction of these surfaces (the solution in the large) is integral to the feedback solution of the game and the verification of the saddle point inequalities. The feedback solution is discussed further later on.

The ETM concept has been generalized and extended to other payoff functions and fan (sector)-shaped capture sets in [24], and to three-dimensional encounters in [28].

3. CONSTRUCTION OF AIRCRAFT ETMs

The general behaviour of the extremals in the ETM can be deduced from the necessary conditions coupled with numerical experience with the aircraft model F-4C used earlier [23, 24, 27]. The ETM is symmetric with respect to the x-axis with extremals for positive and negative values of β_f forming mirror images. For $\beta_f = 0^\circ$, the extremal is the full-throttle level flight path along the negative x-axis.† For β_f values below β_l, where

$$\beta_l = \arctan(2C/f\mathrm{M}) \tag{12}$$

the bank control ω starts out partial and increases in retrograde time until saturation. Once ω saturates, the throttle may later be switched to zero if the Mach number is above the corner velocity M ($=0.88$ for F-4C) where the instantaneous turn rate attains its maximum. When β_f increases beyond β_l, the extremals emerge with full bank. All full-bank segments of the extremals are generated using trajectory templates (prestored long duration trajectories flown at full bank) [23]. For $\beta_f > 90^\circ$, the terminal controls are full-bank and zero throttle. In the range 90°–100° for β_f, the throttle may be switched to full and back to zero in retrograde time. If an extremal intersects the x-axis with $\mathrm{p_M} > 0$, ω switches sign according to (10). If however, $\mathrm{p_M} < 0$ as the extremal approaches the x-axis, then (9) holds and ω changes sign gradually. This happens for $\mathrm{M}_f < \hat{\mathrm{M}}$.

Since the Hamiltonian is linear in Π, intermediate values of Π are singular controls. For F-4C, partial thrust and zero bank arcs are optimal only at the upper speed bound ($\bar{\mathrm{M}} = 1.6$). Partial-thrust full-bank singular arcs are not encountered in the computations.

An example ETM for $\mathrm{M}_f = 1.3$ at an altitude of 6.1 km is reproduced from [23] as Fig. 3. The values of β_f are marked along the extremals. The throttle switching and bank saturation curves are also shown. An alternative representation of ETM as a set of extremals for fixed initial M_0 and time-to-go τ ($= t_f - t_0$) is used in [27].

Suboptimal approximations to the extremals are generally considered for analysing the effect of suboptimal play or to reduce computations without significantly affecting the performance. Figure 4 (reproduced from [24]) shows the ETM for F-4C flying at the same altitude of 6.1 km but at a fixed speed of $\mathrm{M} = 0.8$. The minimum turn radius of the aircraft here is 1.468 km. This was constructed to study the effect of such a constraint. The same reference shows the ETM for the same aircraft with three-level bank control ($\omega = +1, 0, -1$ only) as a reasonable approximation to the true ETM.

†The subscript i is dropped on ETM variables in this section.

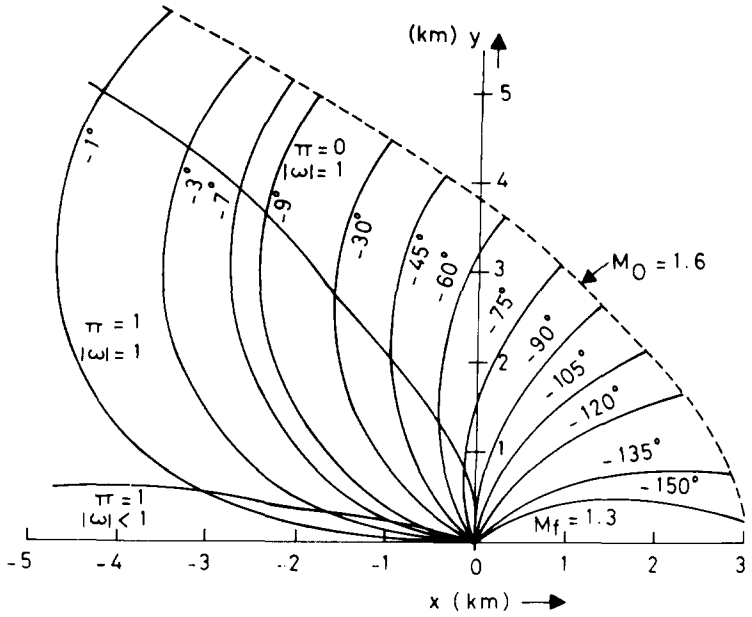

Fig. 3. ETM for constant altitude pursuit–evasion. Altitude = 6.1 km. β_f is marked along the curves.

Reference [27] presents several insights and approximations applicable in the construction of extremals to meet certain speed change, turn angle, and time-to-go requirements for a given initial speed M_0. In particular, for extremals with time-to-go over 20 s, zero-throttle arc segments are small and can be safely ignored. Since extremals with turn angle much more than 180° are found to go beyond Dispersal surfaces in the feedback solution of the game, extremals lasting longer than 20 s necessarily have partial bank segments and end up with $\beta_f < \beta_l$. As the duration of the extremal increases, the terminal heading β_f tends to zero and the terminal Mach number M_f increases to $\bar{M}$. Once M_f reaches $\bar{M}$, the extremals consist of an initial accelerating turn to $\bar{M}$ followed by a cruise arc comprising a very short duration circular arc and a straight dash both at $\bar{M}$. The possibility of approximating intermediate-duration extremals (which do not exhibit cruise arcs) by separating them into turning and accelerating phases are also explored in depth. The long duration extremals with cruise arcs are characterized by a single parameter, the heading change on the cruise arc.

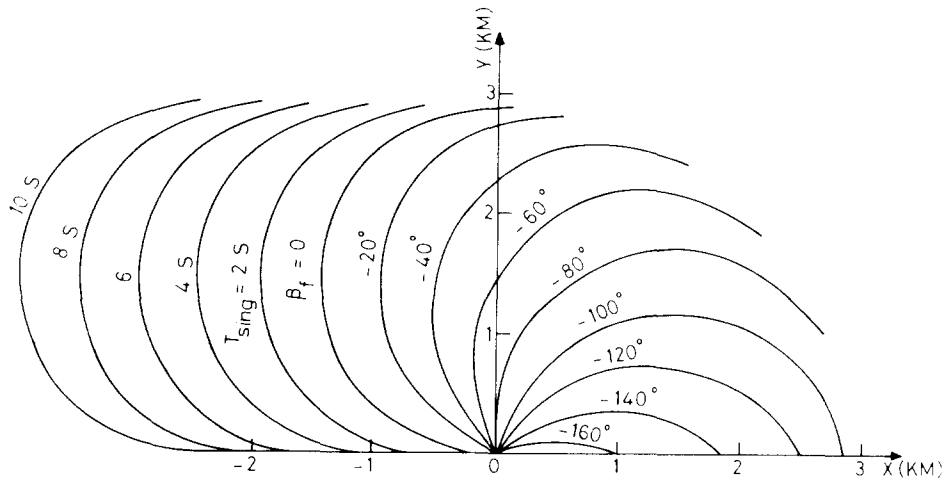

Fig. 4. ETM for constant speed aircraft model.

4. THE FEEDBACK SOLUTION

It is seen that the ETM of an aircraft is a collection of all possible time-optimal paths that the aircraft may use in any pursuit–evasion–interception encounter against an adversary. However, any given pair of extremals, taken one each from the ETMs of two adversaries, need not lead to an optimal encounter in a saddle point sense. First, the reachability condition on the relative velocity at termination (11) may not be met. A reversal of the inequality (11) indicates nonusability of the termination. If, however, (11) is satisfied as an equality, putting together of the two extremals generates a path on the Barrier. The Barrier is a singular surface on which the normality condition is not met. Depending upon whether it is open/closed, it separates the relative evader positions corresponding to easy and more involved/impossible capture. Secondly, even if the reachability condition is met, the game trajectory in the reduced space generated by the extremals is optimal only until a Dispersal surface for one of the aircraft is encountered. Beyond the Dispersal surface, this aircraft will have a better extremal to use. The construction of the Barrier and Dispersal surfaces is thus inherent to the feedback solution.

Apart from the Barrier and Dispersal surfaces, the feedback solution must present the control switching surfaces carving the Capture zone into regions within which the control strategies are constant. Corresponding to the bank control which varies continuously over certain portions of the extremals, constant control-value surfaces need to be mapped. Since all these surfaces are in a reduced state space of dimension five or four (the latter case when one of the aircraft flies at a fixed speed), they can only be pictured by cross sectioning. They are sectioned by keeping constant the initial Mach numbers of the pursuer and evader (M_{p_0}, M_{e_0}) and their initial relative heading

$$\beta_0 = \beta_{p_0} - \beta_{e_0} \tag{13}$$

The cross sections for various sets of section parameters (M_{p_0}, M_{e_0}, β_0) are plotted as curves relative to the pursuer in the plane of the encounter.

In the direct iteration method, it is first noted that points on the switching surface of an aircraft are parametrized by the values of that aircraft's β_f. An iterative search on the remaining terminal parameters is carried out to satisfy the conditions characterizing the surface and the parameters M_{p_0}, M_{e_0}, β_0 of the section. Once the search is completed, the relative position coordinates are used to map the point on the section. This is explained in [23, 25].

For instance, the bank switching surface of the pursuer corresponds to the x-axis in its ETM. Its (M_{p_0}, M_{e_0}, β_0) section is constructed as follows. For a given value of β_{p_f}, a value of M_{p_f} is searched in its ETM such that M_p becomes M_{p_0} at some retrograde time τ_0, when the extremal cuts the x-axis. The evader's terminal velocity vector is then searched such that (11) is met and at the same τ_0, the M_{e_0}, β_0 conditions are met on the corresponding extremal. Thus, construction of aircraft switching surfaces requires one-dimensional searches in own aircraft's ETM and corresponding two-dimensional searches in the opponent's ETM.

Constant bank-level surfaces are constructed similarly. In the case of Barrier sections, the condition for the boundary of the usable part [given by (11) with an equality sign] relates β_{e_f} in terms of β_{p_f}. A two-dimensional search on M_{p_f}, M_{e_f} is needed to match the initial speeds at the retrograde time when β_0 value is met.

Once the required iterative searches parametrized by β_f values are completed, the relative position coordinates are calculated for the assumed roles and capture radius R. Since this is a direct calculation based on the ETM coordinates, parametric studies for different values of R and interchange of roles need very little additional effort. The implications of this on aircraft design and weapon radius tradeoff are obvious.

An alternative to the direct iteration method of constructing the feedback solution is to locate the Barrier, Dispersal and constant-level points on the (M_{p_0}, M_{e_0}, β_0) cross sections of the isochrones (constant optimal-time loci) for different times-to-go. A control-level surface links the points on the isochrones at which the controls take on a specified value. Dispersal points are located at the intersections of different branches of the same isochrone. Where the isochrone cross sections are not closed, their end points are on a Barrier cross section. The construction of the isochrone sections for different (M_{p_0}, M_{e_0}, β_0) values leads to a mapping of the game surfaces. This method has been elucidated in [26, 27].

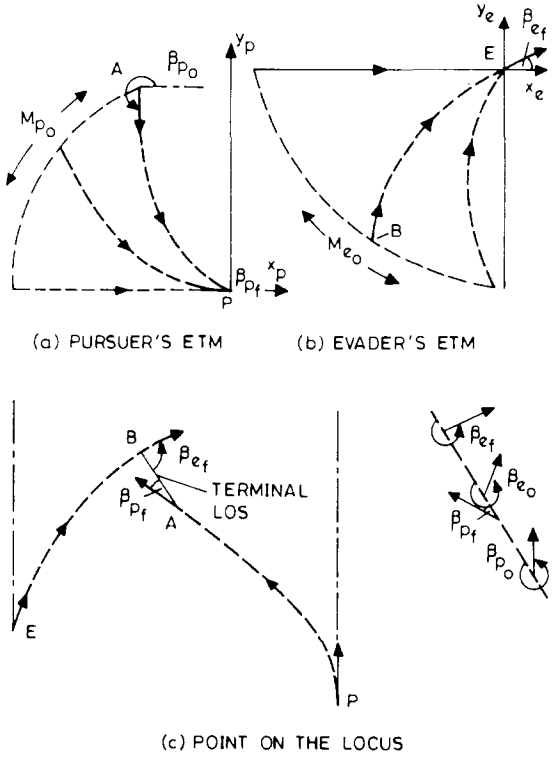

Fig. 5. Construction of a point on an isochrone.

Figure 5(a) and (b) shows the pursuer and evader ETMs in which all the extremals are generated for the same time-to-go and fixed initial Mach numbers M_{p_0}, M_{e_0} with β_{p_f}, β_{e_f} as parameters. The isochrone section being constructed has β_0 also specified in addition to M_{p_0}, M_{e_0}. For any pair of headings β_{p_f}, β_{e_f}, the terminal M_{p_f}, M_{e_f} have already been searched to match the starting M_{p_0}, M_{e_0}. For matching the β_0 value, β_{p_f} is considered fixed and β_{e_f} is searched in the evader's ETM. Figure 5(c) shows the construction of a point on the isochrone section. Searching in the evader's ETM is unnecessary in the interception problem since the target's turn angle over the engagement time is independent of its terminal heading and is known in advance [26].

5. SOME EXAMPLES

References [23–27] present a variety of examples of pursuit–evasion–interception encounters between two aircraft and map the Barriers and Dispersal points for the game. The aircraft models are taken as that of F-4C at an altitude of 6.1 km and capture radius R as 316 m corresponding to engagement with guns. In particular, Barrier sections for the four-dimensional game in which one of the aircraft is constrained to fly at a sustained speed of M = 0.8 are given in [25]. The case of both aircraft varying their speeds is considered in [23]. The isochrone method is exploited in [26, 27]. The former considers the interception problem while the latter the pursuit–evasion problem also.

Figure 6 reproduces the Barrier sections for an initially face-to-face encounter ($\beta_0 = \pm 180°$) in which it is the pursuer that uses a sustained speed of M = 0.8. The evader's initial Mach number is marked on the sections. The corners in each of the sections indicate the Dispersal points. The sections are closed for the obvious reason that if the evader is sufficiently far away, he can speed up to Mach 0.8, and then out-turn and out-dash the pursuer. Points on the head-on (upper) dispersal curve result in left–right mirror-symmetric trajectories for the evader. There are two other Dispersal curves on the sides. For points on these curves, the evader has a choice between two different trajectories to either out-turn or out-dash the pursuer. The latter type of Dispersal curves merge with the symmetric dispersal curve and disappear once the evader Mach number exceeds 0.7. The area of the Barrier sections decreases as the evader's initial speed increases. This trend

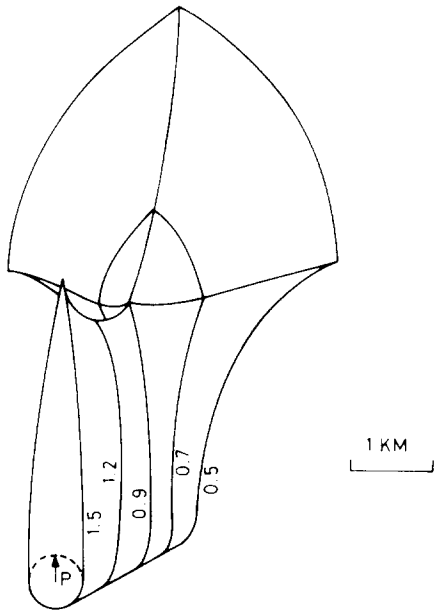

Fig. 6. Sustained speed pursuit vs variable speed evasion – Barrier sections (face-to-face case).

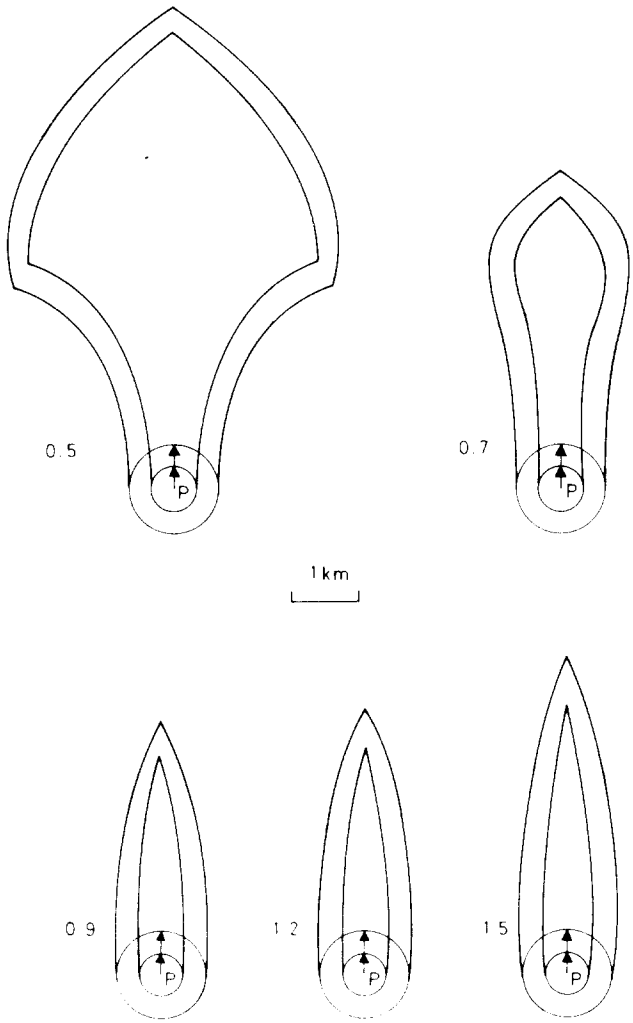

Fig. 7. Comparison of Barrier sections for different values of capture radius.

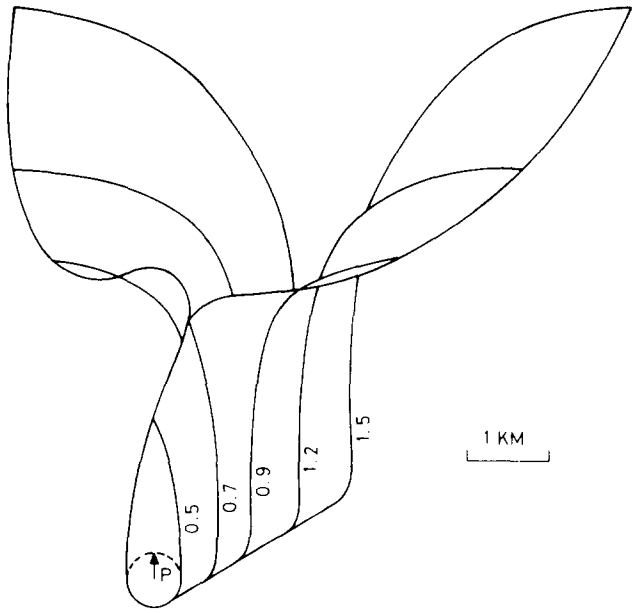

Fig. 8. Variable speed pursuit vs sustained speed evasion—Barrier sections (face-to-face case).

reverses somewhat when increase in evader's speed capability is counterbalanced by his reduced turn rate.

Figure 7 compares the Barrier sections for different values of capture radius ($R = 316$ and 632 m). Figure 8 represents the Barrier sections for initially face-to-face encounters with the reversed roles. The evader flies at a sustained speed of M = 0.8. The pursuer's initial Mach number is marked across the sections. The Barrier tears and opens up for pursuer speeds above M = 0.7. Clearly, there is no escape zone for the evader in this case. For pursuer initial speeds smaller than M = 0.7, relatively small regions of relative evader positions only result in easy capture. The evader almost runs into the pursuer due to turn rate restrictions. This region expands up for higher pursuer

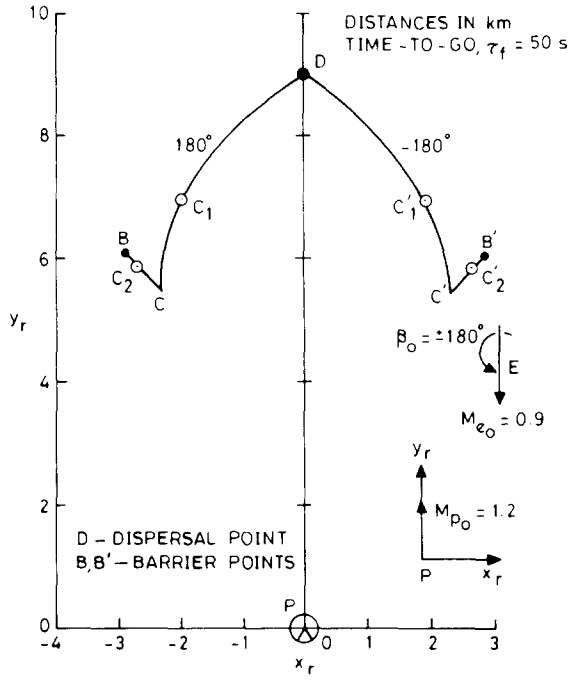

Fig. 9. An isochrone section for pursuit-evasion.

initial speeds. Figures 7 and 8 are produced from the same iterative searches required for drawing Fig. 6.

Barrier sections for the case when both (identical) aircraft vary their speeds [23] do not show the ice-cream cone shaped bulges of Fig. 6 or the open shaped Barrier of Fig. 8. The Dispersal points are also of the symmetric type only. These phenomena occur only when one of aircraft plays suboptimally by restraining its speed at a fixed value.

An isochrone section for pursuit–evasion is reproduced from [27]. The initial speeds of the pursuer and evader are M = 1.2 and 0.9 respectively. The capture radius is 316 m. The time-to-go is 50 s and the aircraft are initially face-to-face. The symmetric Dispersal point is depicted at D and the left and right Barrier points at B, B′. From D to B, the pursuer's turn angle increases, and its terminal speed M_f and distance traversed fall; the reverse is true for the evader. The distance traversed by both aircraft is approximately the same at C, which is the point nearest to the pursuer on the locus. The encounters starting from C_1 and C are symmetric in that the turn angles of the pursuer and evader at C_1 are almost the opposite to those at C. At C_1, the encounter terminates at a position beyond the evader's initial position (increasing y). The distance traversed by the pursuer decreases and that by the evader increases in the direction C_1CC_2. For capture in the same time, the evader must, therefore, start closer to the pursuer and the points on the segment C_1C are in fact nearer to P. At C, the encounter terminates behind the pursuer's initial position. For capture in the same time, the points to the left of C must be farther away from P than C, which explains the kink in the isochrone at C.

6. CONCLUSIONS

The ETM is a convenient concept for an aircraft to represent its pursuit–evasion–interception capability against any adversary. Approximations to the extremals can be studied to explore the effect of suboptimal play and/or to reduce computations without significantly affecting the performance. Since a range of parametric studies with different values of weapon radius and reversal of roles can be carried out with ease using ETMs, it has potential for exploitation in design studies to evaluate different aircraft configurations and weapon systems against a specific threat aircraft.

REFERENCES

1. R. Isaacs, *Differential Games*. Wiley, New York (1965).
2. A. W. Merz, The game of two identical cars. *J. Optim. Theory Applic.* **9**, 324–343 (1972).
3. U. H. D. Lynch, Differential game barriers and their application in air-to-air combat. Ph.D. dissertation, DS/MD/73-1, Air Force Institute of Technology, Wright Patterson Air Force Base, Ohio (1973).
4. G. J. Olsder and J. V. Breakwell, Role determination in an aerial dogfight. *Int. J. Game Theory* **3**, 46–47 (1974).
5. W. Y. Peng and T L. Vincent, Some aspects of aerial combat. *AIAA J.* **13**, 7–11 (1975).
6. H. J. Kelley and L. Lefton, Estimation of weapon radius vs maneuverability tradeoff for air-to-air combat. *AIAA J.* **15**, 145–148 (1977).
7. J. V. Breakwell and A. W. Merz, Minimum required capture radius in a coplanar model of the aerial combat problem. *AIAA J.* **15**, 1089–1094 (1977).
8. A. W. Merz and D. S. Hague, Coplanar tail-chase aerial combat as a differential game. *AIAA J.* **15**, 1419–1424 (1977).
9. A. W. Merz, To pursue or evade—that is the question. *J. Guid. Control Dynam.* **8**, 161–166 (1985).
10. D. A. Roberts and R. C. Montgomery, Development and application of a gradient method for solving differential games. NASA Report TND-6502 (1971).
11. G. M. Anderson, W. L. Othling and S. M. D. Williamson-Noble, The dynamic modeling technique for obtaining closed-loop control laws for aircraft/aircraft pursuit–evasion problems. *Proceedings of the Joint Automatic Control Conference*, Stanford University, pp. 953–954 (1972).
12. A. L. Leatham and U. H. D. Lynch, Two numerical methods to solve realistic air-to-air combat differential games. AIAA Paper 74-22, Washington, D.C. (1974).
13. G. M. Anderson, A near-optimal closed-loop solution method for nonsingular zero-sum differential games. *J. Optim. Theory Applic.* **13**, 303–318 (1974).
14. B. S. A. Jarmark, Near-optimal closed-loop strategy for aerial combat games. Department of Automatic Control, The Royal Institute of Technology, Stockholm, Sweden (1976).
15. H. J. Kelley and L. Lefton, Differential turns. *AIAA J.* **11**, 858–861 (1973).
16. H. J. Kelley, Differential turning optimality criteria. *J. Aircraft* **12**, 41–44 (1975).
17. H. J. Kelley, Differential turning tactics. *J. Aircraft* **12**, 930–936 (1975).
18. H. J. Kelley and L. Lefton, Calculation of differential turning barrier surfaces. *J. Spacecraft Rockets* **14**, 87–95 (1977).
19. J. Shinar, Validation of zero-order feedback strategies for medium-range air-to-air interception in a horizontal plane. NASA TM-84237 (1982).

20. N. Farber and J. Shinar, An approximate feedback solution of a variable speed nonlinear pursuit–evasion game between two airplanes in a horizontal plane. AIAA Paper 80–1597 (1980).
21. J. Shinar and N. Farber, Horizontal variable-speed interception game solved by forced singular perturbation techniques. *J. Optim. Theory Applic.* **42,** 603–636 (1984).
22. M. Ardema and N. Rajan, Slow and fast state variables for 3-D flight dynamics. *J. Guid. Control Dynam.* **8,** 532–535 (1985).
23. N. Rajan, U. R. Prasad and N. J. Rao, Pursuit–evasion of two aircraft in a horizontal plane. *J. Guid. Control* **3,** 261–267 (1980).
24. U. R. Prasad, N. Rajan and N. J. Rao, Planar pursuit–evasion with variable speeds, Part 1: extremal trajectory maps. *J. Optim. Theory Applic.* **33,** 401–418 (1981).
25. N. Rajan, U. R. Prasad and N. J. Rao, Planar pursuit–evasion with variable speeds, Part 2: barrier sections. *J. Optim. Theory Applic.* **33,** 419–432 (1981).
26. N. Rajan and M. D. Ardema, Barriers and dispersal surfaces in minimum-time interception. . *Optim. Theory Applic.* **42,** 201–228 (1984).
27. N. Rajan and M. D. Ardema, Optimal feedback strategies for pursuit–evasion and interception in a plane. NASA TM-84311 (1983).
28. N. Rajan and U. R. Prasad, The extremal trajectory map: a new representation of combat capability. AIAA Atmospheric Flight Mechanics Conference, Paper 79-1622 (1979).